This manuscript has been published online in: Journal of Dentistry 2020 May
https://doi.org/10.1016/j.jdent.2020.103359

Title: *Ex vivo* investigations on bioinspired electrospun membranes as potential biomaterials for bone regeneration.

Authors:
R. Osorio[1], A. Carrasco-Carmona[1], M. Toledano[1]*, E. Osorio[1], A.L. Medina-Castillo[2], L. Iskandar[3], A. Marques[3], S. Deb[3], M. Toledano-Osorio[1].

1 University of Granada, Faculty of Dentistry, Dental Materials Section.
Colegio Máximo de Cartuja s/n
18071 – Granada - Spain.

2 University of Granada, NanoMyP. Spin-Off Enterprise.
Edificio BIC-Granada. Av. Innovación 1.
18016 - Armilla, Granada, Spain.

3 Faculty of Dentistry, Oral & Craniofacial Sciences.
King's College London.
London Bridge, London SE1 9RT, UK.

Corresponding author:
Manuel Toledano
Campus de Cartuja s/n
Dental School
University of Granada
E-18071 Granada
SPAIN
E-mail: toledano@ugr.es

Title:

Ex vivo investigations on bioinspired electrospun membranes as potential biomaterials for bone regeneration.

Abstract

Objectives: To assess the surface characteristics and composition that may enhance osteoblasts viability on novel electrospun composite membranes (organic polymer/silicon dioxide nanoparticles).
Methods: Membranes are composed by a novel polymer blend, the mixture of two hydrophilic copolymers 2-hydroxyethylmethacrylate-co-methylmethacrylate and 2-hydroxyethylacrylate-co-methylacrylate, and they are doped with silicon dioxide nanoparticles. Then the membranes were functionalized with zinc or doxycycline. The membranes were morphologically characterized by atomic force and scanning electron microscopy (FESEM), and mechanically probed using a nanoindenter. Biomimetic calcium phosphate precipitation on polymeric tissues was assessed. Cell viability tests were performed using human osteosarcoma cells. Cells morphology was also studied by FESEM. Data were analyzed by ANOVA, Student-Newman-Keuls and Student t tests ($p<0.05$).
Results: Silica doping of membranes enhanced bioactivity and increased mechanical properties. Membranes morphology and mechanical properties were similar to those of trabecular bone. Zinc and doxycycline doping did not exert changes but it increased novel membranes bioactivity. Membranes were found to permit osteoblasts proliferation. Silica-doping favored cells proliferation and spreading. As soon as 24h after the seeding, cells in silica-doped membranes were firmly attached to experimental tissues trough filopodia, connected to each other. The cells produced collagen and minerals onto the surfaces.
Conclusions: Silica nanoparticles enhanced surface properties and osteoblasts viability on electrospun membranes.
Clinical significance: The ability of silica-doped matrices to promote precipitation of calcium phosphate, together with their mechanical properties, observed non-toxicity, stimulating effect on osteoblasts and its surface chemistry allowing covalent binding of proteins, offer a potential strategy for bone regeneration applications.

1. Introduction

Alveolar bone healing post periodontal regeneration or teeth extraction usually takes 6-12 months and often the use of resorbable tissue engineered matrices to induce bone formation is unpredictable [1]. Most resorbable membranes (e.g. collagen, polylactide-co-glycolide, polycaprolactone) and bone graft substitutes (e.g. hydroxyapatite and other calcium phosphates) show a relatively fast rate of biodegradation [1,2] and are unable to exert spatio-temporal control over the wound-healing process [2]. Despite the advantages of resorbable membranes that do not require secondary surgery for their removal (reducing the risks of infection and less tissue damage associated with membrane removal) [2], the durability of these barrier materials over the healing period decreases rapidly. Moreover, some degradation products of these resorbable materials generating a low pH environment that could also alter the remineralization processes [1,3]. Hence engineering materials resembling the native bone structure is important [1], therefore biomaterials with nanostructures, interconnected porous randomized mesh, with assembled fibers are design parameters that enhance bone healing in this region [4].

Presently, non-resorbable synthetic membranes of polytetrafluoroethylene (PTFE), continue to still represent the gold-standard for clinicians, due to its higher predictability in comparison to resorbable membranes [5]. However, PTFE is associated with significant disadvantages: *i)* low adhesiveness for plasma proteins and cells, *ii)* total absence of ability to connect to bone tissue and osseointegration, non-formation of a connective tissue interlayer; a second surgery is required to remove the non-integrated membrane, iii) frequent infections due to lack of antibacterial properties [6], and finally iv) inadequate topography resembling bone tissue.

There is a distinct lack of non-resorbable biomaterials with appropriate properties as an alternative to PTFE membranes. In a previous study we reported methyl acrylate based membranes loaded with calcium or zinc ions that showed potential in periodontal regeneration [7]. To enhance hydrophilicity, cell-membrane interactions, mechanical properties, osteogenic and confer antibacterial properties, a novel composite membranes based on the electrospun of a mixture of $(MMA)_1$-co-$(HEMA)_1$ and $(MA)_3$-co-$(HEA)_2$ doped with silicon dioxide nanoparticles (SiO_2-NPs) are proposed. The composite membranes were formed with silica nanoparticles and functionalized with zinc or doxycycline to enhance osteoblasts viability and proliferation [8], increase rate of new bone formation [9] and inhibit the biofilm formation and the protein synthesis in microbial organisms [10] by virtue of zinc ions and doxycycline respectively. The new composite membranes should combine both the mechanical properties of polymeric materials (very high abrasion resistance, high flexibility, high elasticity, high stress resistance) and the properties of SiO_2-NPs (bioactivity).

The aim of the study was to analyse surface characteristics (topography, nanomechanical properties, bioactivity) and cell viability on silicon dioxide composite membranes functionalized with zinc and doxycycline. The null hypothesis is that SiO_2-NPs and zinc or doxycycline addition on membranes does not affect their topography, nanomechanical properties and osteoblasts viability.

2. Materials and methods

2.1.Preparation of artificial tissues

Nanostructured membranes were manufactured by NanomyP® (Granada, Spain) using a novel polymer blend: $(MMA)_1$-co-$(HEMA)_1$/$(MA)_3$-co-$(HEA)_2$ doped with 5 % wt of SiO_2-NPs. To activate the surface of the membranes whit carboxyl groups (HOOC-Si-membrane) they were immersed into a sodium carbonate buffer solution (333 mM; pH=12.5) for 2 h (due to the partial hydrolysis of ester bonds, carboxyl groups were disposed on their surfaces [11]); then membranes were gently washed with distilled water and dried in a vacuum oven [7]. The ability of carboxyl groups to complex divalent cations was used to functionalize the membranes with zinc. Doxycycline was bound non-covalently into membranes by base-acid interactions between amino groups of Dox and carboxyl groups of the membranes. To control the functionalization degree the adsorption isotherms of Zn^{2+} and Dox on the HOOC-Si-membrane were studied. To do so, HOOC-Si-membranes were incubated at room temperature and under continuous shaking in different aqueous solutions (pH=7) of both $ZnCl_2$ and Dox: 30, 80, 130, 180, 230, 280, 330, 380mgL^{-1} of $ZnCl_2$; and 100, 200, 400, 600, 800, 1000 mgL^{-1} of Dox). Four different membranes were tested: 1) Non functionalized and SiO_2-NPs undoped membrane (HOOC-Membrane), 2) SiO_2-NPs doped membrane (HOOC-Si-Membrane), 3) SiO_2-NPs doped membrane functionalized with Zn (Zn-HOOC-Si-Membrane) and 4) SiO_2-NPs doped membrane functionalized with Dox (Dox-Si-Membrane).

2.2. Atomic force microscopy (AFM) surface characterization

The imaging process was undertaken in the tapping mode, using an AFM (Nanoscope V, Digital Instruments, Veeco Metrology group, Santa Barbara, CA, USA) with a calibrated vertical-engaged piezo-scanner. A 10-nm-radius silicon nitride tip was attached to the end of an oscillating cantilever that came into intermittent contact with the surface at the lowest point of the oscillation. Changes in vertical position of the AFM tip at resonance frequencies near 330 kHz provided the height of the images registered as bright and dark regions. Three specimens of each experimental group were analysed. Three 20 x 20 μm digital images were recorded from each surface, with a slow scan rate (0.1 Hz). Measurements were performed in a wet cell, under hydrated conditions. For each image, five randomized boxes (5 μm × 5 μm) were created to examine surface nanoroughness (SRa, in nanometer) [7]. Roughness was measured using specific software (Nanoscope Software version V7). Fiber diameters and fiber to fiber distances ranges were analyzed with *Image J* software (ImageJ B, National Institutes of Health, Bethesda, Maryland, USA). ANOVA and Student-Newman-Keuls multiple comparisons were performed ($p<0.05$).

2.3. Acellular static in vitro bioactivity test

Three specimens of each experimental group were analysed. Membranes were soaked in 20 ml of simulated body fluid solution (SBF) [pH 7.45] in sterile flasks for 7 days [12]. Reagents per 1000 ml of SBF were: 8.035 g of NaCl, 0.355 g of $NaHCO_3$, 0.225 g of KCl, 0.231 g of $K_2HPO_4 \cdot 3H_2O$, 0.311 g of $MgCl_2 \cdot 6H_2O$, 39 g of 1M HCl,0.292 g of $CaCl_2$, 0.072 g of Na_2SO_4, 118 g of Tris, 0 to 5 ml of 1M HCl for final pH adjustment. After drying and carbon covering, surfaces were analyzed by Field Emission Electron Microscopy (FESEM) (GEMINI, Carl Zeiss SMT, Germany) at 3 Kv, 4.7 to 4.9 mm working distance. Elemental analysis was done by means of an

energy dispersive analysis system (EDX) (Inca 300 and 350, Oxford Instruments, Oxford, UK).

2.4. Nanomechanical properties assessment

Nanomechanical properties mappings were conducted using a Hysitron Ti Premier nanoindenter (Hysitron, Inc., Minneapolis, MN) equipped with nano-DMA III, a commercial nano-DMA software. Modulus mapping of the samples was done by imposing a quasi-static force setpoint, F_q=2 μN, to which a sinusoidal force of amplitude F_A=0.10 μN and frequency *f*=200 Hz was superimposed. The resulting displacement (deformation) at the site of indentation was monitored as a function of time. Three specimens of each experimental group were analysed. Data from three regions, of each specimen, approximately 20×20 μm in size were collected using a scanning frequency of 0.2 Hz. Specimens were scanned under a hydrated state [7]. Under steady conditions (application of a quasistatic force) the indentation modulus of the tested sample, *E*, could be obtained by application of different models that relate the indentation force, *F*, and depth, *D* [13]. Most of these theories assume proportionality between the force and the indentation modulus. Complex modulus (*E**), loss modulus (*E*), storage modulus (*E′*) (GPa) and tan delta (δ) were calculated. The data were analyzed using ANOVA and Student-Newman-Keuls multiple comparisons ($p<0.05$).

2.5. In vitro cytocompatibility

HOS TE85 human osteosarcoma cells line were cultured using Alpha-modified Eagle's medium (Biosera, UK), 10% FBS, and 1% Penicillin/Streptomycin. Cells were grown in membranes culture T75 flask at 37 °C and 5% CO2 in an incubator to 90% confluency. After every 2–3 days, the media was replenished, and cells were passaged (Passage~7) with trypsin-EDTA (Sigma-Aldrich, UK).

Cell proliferation: The membranes were sterilized by gamma irradiation at a dose of 31.8 kGy. Cell proliferation was determined using the Alamar-Blue™assay (Life technologies) which is a redox indicator that measures proliferation quantitatively. Absorbance was read on a fluorescent plate reader on emission wavelength of 590 nm (excitation wavelength 560 nm) [14]. Cells were micro seeded at a total density of 1.6×10^6 cell per membrane (8x8mm) and placed in a 48 well plate. The time period studied were 1, 3, and 7 days. Experiments were performed in triplicate.

Cell Field Emission Scanning electron Microscopy (FESEM) analysis: In order to study cell morphology, two membranes of each experimental group were cultured with cells and utilized for FESEM (GEMINI, Carl Zeiss SMT, Germany) observation. The time-points were 24 h, 7 and 14 d. Samples were submitted to critical drying point and carbon covering.

Cell viability: Three membranes for each experimental group were used and cell viability was analysed using a Live/dead viability/cytotoxicity kit LIVE/DEAD® commercial kit (Life Technologies, Carlsbad, CA, USA). Cells were incubated for 24 or 48 h with 1μM of calcein AM and 2μM of ethidium homodimer in PBS and placed in CO_2 incubator for 20 mins. Calcein stains the live cells green due to intracellular esterase activity, and ethidium stains the cells red as it enters cells with damaged membranes and becomes fluorescent upon binding to nucleic acids in the dead cell [7]. The cells were imaged with a fluorescence microscope (Nikon Eclipse 90i, Nikon, Japan).

Statistical analysis: For cell proliferation and cell viability results two-way ANOVA including analysis of interactions were performed. As interactions between membranes type and time-points were significant, the variables were analyzed

separately. Student-Newman-Keuls multiple comparisons and Student *t* tests were performed to ascertain differences between membranes and time-points ($p<0.05$).

3. Results

3.1. Functionalization of synthetic membranes with Zinc and Dox

Zinc and doxycycline isotherms are shown in Fig. 1. The maximum zinc adsorption of 3 μg Zn/mg membrane was attained when immersed in 330 $[ZnCl_2]_0$ mgL^{-1}, for 60 minutes whilst Dox adsorption at a maximum of 76.2 μg Dox/mg membrane was obtained when immersed in 800 $[Dox]_0$ mgL^{-1} for 30 min.

3.2. Atomic force microscopy surface characterization

There were no significant differences in surface roughness (272.95nm, SRa), mean pore sizes (6.93nm) and pore proportions (0.33) between the groups, however differences were observed in fiber diameter as demonstrated in Table 1.The diameter a for fibers from both the Si-loaded and zinc doped membranes (854.90 nm) were found to be greater than other groups. Representative AFM images of each experimental group are displayed in Fig. 2.

3.3. Acellular static in vitro bioactivity test

Representative FESEM images of the membranes after immersion in SBF for 7 days are shown 7 in Fig. 3. Irregular spherical deposits rich in calcium and phosphate were scattered onto the experimental membranes however the HOOC-membranes lacked these deposits. The presence of silica contributed to the bioactivity whilst presence of doxycycline and zinc doping resulted in greater mineral deposits.

3.4. Nanomechanical properties

The native membrane (HOOC-Membrane) exhibited lowest value of complex modulus, loss modulus and storage modulus (7.7 GPa, 3.29 GPa and 5.70 GPa, respectively) whilst the presence of silica enhanced the mechanical properties (Table 2). The zinc and doxycycline functionalized membranes attained the highest values of complex modulus (22.10 and 17.86 GPa, respectively) whereas the loss modulus values were low for the unloaded membrane and the one functionalized with doxycycline (3.9 and 3.26 GPa, respectively). The native membrane had the maximum tan δ value (0.97), approximately two-fold higher than the other membranes. The mappings from the different experimental membranes are shown in Fig. 4.

3.5. In vitro cytocompatibility

Proliferation assay results of HOS cells cultured on the scaffolds on days 1, 3 and 7 are shown in Fig. 5. Results indicate lower proliferation values for the HOOC-membranes at all time-points and decreased considerably at day 7. In general, there was a low cell viability decrease over time for the rest of the membranes/scaffolds but they were only significant between the first and the third day.

The HOS cells were able to attach on the test membranes and examination of the integrity of the cytoplasmic esterase function and cell membrane integrity with the LIVE/DEAD® cell viability assay, cell viability was recorded above 90% in all the scaffolds (Table 3).

The FESEM analysis indicated that silica-doped membranes enhanced cell adhesion and spreading. Representative FESEM images are presented in Fig. 6, cell adhesion was apparent with collagen formation even at 24h. Groups of connected cells

were observed. Cell development and extended filopodia were also observed, these cytoplasmic extensions were formed profoundly on the rough membrane's surfaces (Figs. 6d, 6h). At high magnification, individual osteoblasts were shown to be connected by tight junctions to neighbor cells, being difficult to be distinguished one from the other (Figs. 6d, 6j). After 7 days culture, osteoblasts were difficult to be observed, as they were almost completely covered by new fiber formation (Figs. 6b, 6f, 6i, 6l). Mineral clusters were also observed, with tiny crystals scattered onto the cell membrane (Figs. 6b, 6f, 6i, 6l) with areas that completely covered the osteoblasts (Figs. 6b, 6i, 6f). All the silica doped membranes supported the HOS cell adhesion and spreading. With the non-silica doped membrane (HOOC-membrane) HOS cells showed (Fig. 6a) fusiform instead of round-shaped and are smaller in size (Fig. 6c) than the rest of the cells that were grown in the presence of silica (Fig. 6).

4. Discussion

Although various scaffolds have been used to facilitate bone regeneration [15–17] during periodontal wound healing, PTFE membranes continue to be the most widely used. To enable and exert control on the complex spatiotemporal events that occur during periodontal healing, this study reports novel composite non resorbable membranes of a hydrophilic copolymer of methylacrylate-hydroxyethyl acrylate doped with silica nanoparticles as filler, and further functionalized with zinc or doxycycline. The membranes were prepared by electrospinning and a multi-parameter characterization was performed: surface topography by AFM (fiber to fiber distances, fiber diameter and roughness), surface mechanical properties, static *in vitro* bioactivity and cytocompatibility using HOS cells [18].

Zinc functionalization of membranes was effective and did not modify their morphology (Figs. 1a, 2). The membrane surfaces contain carboxylic functional groups (COO^-), which were able to complex with zinc ions on immersion in $ZnCl_2$ solution (Fig. 1a), mainly due to the potent chelating effect of carboxyl groups [19], as described in detail, previously [20]. The effective functionalization of membranes with doxycycline (Fig. 1b) is attributed to the water soluble amphoteric compound, doxycycline hyclate, enabling the binding of the carboxylic acid groups on the outer surface of the membranes with the amino group available in doxycycline (primary; RNH_2 and tertiary; R_3N amine); thus its binding on the surface of membranes is carried out by base-acid interactions between the amino groups of Dox and carboxyl groups of membrane and physical adsorption.

Bioactive materials can induce formation of hydroxyapatite precipitates in contact with body fluids, are of great interest for their bone bonding capacity. Bioactivity can experimentally be predicted if Ca/P deposits are formed on the material surface, on immersion in SBF [21]. Silica doping of the membranes promoted biomimetic precipitation of Ca/P deposits (Fig. 3), whilst the non-silica doped membranes also exhibited minor deposition of calcium phosphate. This occurs as the external surface of membranes contain negatively charged carboxyl groups, that allows some complexation with calcium in presence of SBF immersion, and it is hypothesized that calcium on the membranes may then bond ionically to PO_4^{3} ions (in SBF), creating Ca/P deposits (Fig. 3). The phosphate groups at the surface will also have under coordinated oxygen ions, leading to reactive surfaces, which will attract calcium ions from SBF [22]. However, bioactivity was dramatically enhanced after silica-doping of nanofibers and Ca/P rich crystals were found to form on the surface of all silica-doped membranes, as evidenced by FESEM analysis (Fig. 3). It is known that silica plays an

important role in surface bioactivity of silica-based glasses [23]. In the physiological environment or in SBF, silica is largely negatively charged and surface silanols (Si-OH) can be formed, facilitating calcium and phosphate deposition on the surfaces [23].

The present approach consists of using silica nanoparticles as functional molecules, which may selectively induce nucleation of Ca/P, thereby, tuning the chemistry of the nanofibers. Controlling the nucleation of a mineral phase may finally result in creation of hybrid membranes, composed of two different materials (*e.g.* polymers and inorganic compounds) [24]. Biomimetic calcium and phosphate deposition on the tested membranes is crucial in bone regeneration, since they mimic to some extent the structure of natural bone extracellular matrix. Newly formed calcium phosphate compounds at membranes may provide excellent properties as: 1) similar composition to bone; 2) the ability to further form bone apatite-like materials; 3) ability to stimulate osteoblastic lineage cells, leading to bone formation and 4) osteoconductivity [25]. It should also be taken into account, that during bone metabolism, osteoclasts release Ca^{2+} and PO_4^{3-} from the mineralized bone matrix, producing a local increase in these ion concentrations. This plays a determinant role in osteoblast proliferation and differentiation. Thus, the increase in extracellular Ca^{2+} and PO_4^{3-} concentrations are chemical signals for bone cells proliferation and migration [26], and will also favor bone remodeling [27]. It should be considered that crystalline hydroxyapatite present in most commercial bone substitutes is slow to resorb or even does not resorb. However, precipitated nano-apatite does tend to resorb, thereby facilitating hard tissue regeneration. Doping the polymeric membranes prepared by electrospinning with the blend $(MMA)_1$-co-$(HEMA)_1$/$(MA)_3$-co-$(HEA)_2$ with SiO_2-NPs enhanced the nucleation of Ca/P on their surface. Controlling the nucleation of a mineral phase on polymeric membranes may result in the preparation of a new generation of highly bioactive membranes for bone regeneration [24].

Scaffold architecture has been shown to influence cell attachment and migration [28]. Interestingly, the complexation with zinc or doxycycline adsorption onto membranes did not alter the morphology (Fig. 2) but additionally enhanced mechanical properties (Table 2; Fig. 4) and an augmented nano-roughness (Table 1; Fig. 2) were also encountered after silica nanoparticles were loaded onto membranes. Although the differences in nano-roughness were not significant between the membranes; the mean value of 270 nm (Table 1) lies within the range that (50 to 500 nm) selectively enhances protein adsorption contributing to cell attachment [29]. Furthermore, the surface silanols (formed from silica nanoparticles) are expected to bind to functional groups of proteins via hydrogen bonding and electrostatic ionic bonds, which is favorable towards cell attachment [23]. The hydrophilicity of the experimental membranes is also crucial for cell adhesion and proliferation [30], along with nano-roughness values, which are determinant parameters that supposedly enhance non-specific proteins adhesion and cellular attachment to matrices [29]. The membranes also generated similar pore size (6.93 nm) with an ample pore size range from 4.6 to 8.4 nm (Table 1) and previous studies suggest that pores between 5 to 8 microns increase osteogenic differentiation possibilities for cell growth attached to them [28].

The results showed that the mean fiber diameter of the membranes were around 765 nm, even when significant differences were found between the experimental membranes; these numerical differences are low, under 100 nm (Table 1). This fiber diameter may be considered bone-biomimetic, taking into account that mineralized collagen fibrils are about 800 nm in human trabecular bone and mimicking collagen fibrils diameters have been shown to enhance cell attachment on membranes by about 1.7 fold [29]. The best approach towards an ideal scaffold design mimicking the native

tissue and the fibrillar structure is important for cell attachment, proliferation, and differentiation. The present membranes are bioinspired as they have been designed and developed through inspiration by solutions found in natural collagen from bone. The main goal was to improve modeling and bone simulation of the novel constructs to favor osteoblasts viability and proliferation.

The dynamic nanomechanical properties of the polymeric nanostructured membranes showed that different dynamic complex modulus were obtained for the different membranes: COOH-membrane 7.70±1.69 < COOH-Si-membrane 12.54±2.96 < Zn-Si-membrane 22.10±6.93 = Dox-Si-membrane 17.86±6.60 (in GPa, Table 2, Fig. 4). Complex moduli of loaded and doped (with Zn or Dox) membranes were within the range of the nanoindentation moduli of calcified trabecular bone, which is about 15 to 17 GPa [31]. Recent findings suggest that matrix elasticity (complex modulus) and substrate stiffness may be probed by cells [32], which then modify proliferation and differentiation as a response to differences in mechanics of fibrillar matrices [33]. These membranes, with similar values to those of trabecular bone (CM: 15 GPa; tan δ: 0.6) [31], is thus expected to enhance cell adhesion/spreading, osteoblasts differentiation and proliferation. Since tan δ values higher than 1 represent liquid-like regions and tan δ values lower than 1 represent gel-like behavior [34], the silica-doped experimental membranes should favor cell spreading since the tan δ values ranged from 0.4 to 0.5 (Table 2, Fig. 4) [33].

The membranes have to perform under mechanical stress [1] *in vivo*. Most of recently proposed materials (collagen fibrils, polycaprolactone, polyglicolic acid etc…) exhibit poor mechanical properties compared to the native tissues they are targeted to mimic [35]. Silica doped and functionalized membranes achieved the highest elastic or storage modulus compared with the non-silica doped group (Table 2, Fig. 4). Silica doping is hence important to store potential energy which is released after deformation. Dissipation of energy within the structures is crucial in dynamic systems [36]. Implanted structures in the oral cavity require damping to absorb mechanical shock waves and alleviate stresses. Tan δ measurement permits to calculate the ratio of the dissipated energy by the system, to the stored energy. It will enable its elastic recoil [13], and will provide a general idea of the mechanical behavior of a viscoelastic material [13].

The preliminary results from the *in vitro* cell culture studies did not identify significant necrotic and/or apoptotic effects, of the tested membranes using human osteoblasts (Table 3; Figs. 5, 6). It was not unexpected, as employed polymers in the new blend for membranes manufacturing [i.e. $(MMA)_1$-co-$(HEMA)_1$/$(MA)_3$-co-$(HEA)_2$] are composed by long-chain carbons with hydroxyl (-OH) and methyl (-CH_3) radicals. The only products that may be liberated after partial potential hydrolysis of the polymers are ethanol or propanol, but at a very low and non-toxic concentrations. Moreover, for membranes functionalization, the surface is activated with carboxyl groups, and membranes are immersed into a sodium carbonate buffer solution producing partial hydrolysis of the ester bonds. After this process, the expected release of polymer degradation products due to hydrolysis is negligible. Presented cells proliferation results may be even underestimated; as employed initial cell seeding density was high, and cells were rapidly confluent, as observed at the FESEM images (Figure 6). The results showed that silica-doped membranes were more favorable for cell proliferation in comparison to the group containing no silica nanoparticles. There was a decrease in cell proliferation at day 7, however this was not to the same extent as non Si-NPs membranes and this also illustrates that doxycycline or zinc at assayed concentrations were not cytotoxic (Figs. 5, 6). In addition, previous reports in literature

have shown that silicon is crucial to obtain bone formation and growth, not only *in vitro*, but also *in vivo* conditions [23]. It seems that cells attached on silica-rich surfaces produce higher alkaline phosphatase activity which, implies that silica not only promote cell differentiation, but further the expression of osteoblast phenotype, due to a direct interaction between cells with silica rich surfaces [23]. It has been previously shown that silica-NPs based films can impart bioactivity and biocompatibility to other surfaces, promoting bone ingrowth and differentiation of stem cells into osteoblasts, leading to enhanced osteointegration [8]. The bioinspired topography of these experimental membranes seems to enhance osteoblast adhesion and extracellular matrix formation. In presence of silica, the cells were observed to be bigger in size and round shaped (Fig. 6); indicating major fiber and mineral production activity, as corroborated by FESEM (Fig. 6). However, these membranes will also require relevant experimental animal models for further analysis [18]. It should also be taken into account that chemically and structurally similar membranes have been successfully experimented in a rabbit model with bone healing in calvarial defects [9]. No osteogenic inducing agents were used in the present study and co-culture of osteoblasts and macrophages is the subject of a future study since macrophages have been shown to exert osteogenic activity and to modulate osteoblasts mineralization capacity [37].

The main advantage of the membranes reported in this study alleviates the disadvantages associated with other non-reabsorbable synthetic membranes used in bone regeneration (PTFE membranes). The high silica content, in the experimental membranes, impart a high calcium binding affinity, which is essential for osteoblastic lineage cells differentiation and bone regeneration. Moreover, the incorporation of antibacterial agents may be useful, as sometimes bone regeneration is performed in contaminated oral environments [38]. It is also important to point out that polymer-based scaffolds/membranes loaded with zinc are expected to display enhanced cell proliferation and faster wound healing in bone regeneration, as shown in similar membranes [9]. Moreover, these membranes can be further covalent bonded or biomolecules (enzyme, growth factors, antibody, antigen …) can be immobilized on the surfaces making them a versatile system for many biomedical applications.

Biomaterials mediated inflammatory response is also crucial in bone regeneration. The immune response directly participates in regulating the activities of tissue resident osteoblasts, thereby affecting tissue regeneration outcomes. Excessive inflammation may lead to the formation of a fibrous tissue, preventing the bone cells from integrating with the membranes. This would result in the failure of bone regeneration. A proper inflammatory response may enhance the recruitment and differentiation of osteoblasts, improving osteogenesis. Surface chemistry (hydrophilicity, surfaces with carboxyl groups) and nanotopographies of these membranes could be of great value for immunomodulating bone tissue regeneration [39]. It has been previously stated that these properties may induce macrophage polarization towards M2 (anti-inflammatory) phenotype [39]. Further research is required on immunomodulation and osteogenic differentiation analysis.

5. Conclusions

Silica NPs doping of membranes fabricated by electrospinning did not modify topography but increased nanomechanical properties of the doped membranes. An enhanced bioactivity and osteoblasts proliferation were also encountered in the presence of silica. In general, zinc or doxycycline functionalization did not exert clear differences on the properties investigated. The experimental biomimetic membranes may be considered as a novel potential construct intended for enhancing bone regeneration.

Disclosure

The authors report no conflicts of interest in this work.

Acknowledgements

This work was supported by the Ministry of Economy and Competitiveness (and European Regional Development Fund [Project MAT2017-85999-P MINECO/AEI/FEDER/UE] and University of Granada Research and Transfer Program.

References

[1] M. Sanz, C. Dahlin, D. Apatzidou, Z. Artzi, D. Bozic, E. Calciolari, H. De Bruyn, H. Dommisch, N. Donos, P. Eickholz, J.E. Ellingsen, H.J. Haugen, D. Herrera, F. Lambert, P. Layrolle, E. Montero, K. Mustafa, O. Omar, H. Schliephake, Biomaterials and regenerative technologies used in bone regeneration in the craniomaxillofacial region: Consensus report of group 2 of the 15th European Workshop on Periodontology on Bone Regeneration, J. Clin. Periodontol. 46 Suppl 21 (2019) 82–91. doi:10.1111/jcpe.13123.

[2] N.Y. Naung, E. Shehata, J.E. Van Sickels, Resorbable Versus Nonresorbable Membranes: When and Why?, Dent. Clin. North Am. 63 (2019) 419–431. doi:10.1016/j.cden.2019.02.008.

[3] H. Shimauchi, E. Nemoto, H. Ishihata, M. Shimomura, Possible functional scaffolds for periodontal regeneration, Japanese Dental Science Review. 49 (2013) 118–130. doi:10.1016/j.jdsr.2013.05.001.

[4] W.V. Giannobile, T. Berglundh, B. Al-Nawas, M. Araujo, P.M. Bartold, P. Bouchard, I. Chapple, R. Gruber, P. Lundberg, A. Sculean, N.P. Lang, P. Lyngstadaas, M. Kebschull, P. Galindo-Moreno, Z. Schwartz, L. Shapira, A. Stavropoulos, J. Reseland, Biological factors involved in alveolar bone regeneration: Consensus report of Working Group 1 of the 15th European Workshop on Periodontology on Bone Regeneration, J. Clin. Periodontol. 46 Suppl 21 (2019) 6–11. doi:10.1111/jcpe.13130.

[5] Y.-D. Cho, Y.-J. Seol, Y.-M. Lee, I.-C. Rhyu, H.-M. Ryoo, Y. Ku, An Overview of Biomaterials in Periodontology and Implant Dentistry, Adv. Mater. Sci. Eng. 2017 (2017) 1–7. doi:10.1155/2017/1948241.

[6] G. Sam, B.R.M. Pillai, Evolution of Barrier Membranes in Periodontal Regeneration-"Are the third Generation Membranes really here?", J. Clin. Diagn. Res. 8 (2014) ZE14–ZE17. doi:10.7860/JCDR/2014/9957.5272.

[7] R. Osorio, C.A. Alfonso-Rodríguez, E. Osorio, A.L. Medina-Castillo, M. Alaminos, M. Toledano-Osorio, M. Toledano, Novel potential scaffold for periodontal tissue engineering, Clin. Oral Investig. 21 (2017) 2695–2707. doi:10.1007/s00784-017-2072-8.

[8] L. Andrée, D. Barata, P. Sutthavas, P. Habibovic, S. van Rijt, Guiding mesenchymal stem cell differentiation using mesoporous silica nanoparticle-based films, Acta Biomater. 96 (2019) 557–567. doi:10.1016/j.actbio.2019.07.008.

[9] M. Toledano, J.L. Gutierrez-Pérez, A. Gutierrez-Corrales, M.A. Serrera-Figallo, M. Toledano-Osorio, J.I. Rosales-Leal, M. Aguilar, R. Osorio, D. Torres-Lagares, Novel non-resorbable polymeric-nanostructured scaffolds for guided bone regeneration, Clin. Oral Invest. (2019). doi:10.1007/s00784-019-03068-8.

[10] J. Bueno, M.C. Sánchez, M. Toledano-Osorio, E. Figuero, M. Toledano, A.L. Medina-Castillo, R. Osorio, E. Osorio, D. Herrera, M. Sanz, Antimicrobial effect of nanostructured membranes for guided periodontal regeneration: an in vitro study. (2020).

[11] X. Punet, R. Mauchauffé, J.C. Rodríguez-Cabello, M. Alonso, E. Engel, M.A. Mateos-Timoneda, Biomolecular functionalization for enhanced cell-material interactions of poly(methyl methacrylate) surfaces, Regen. Biomater. 2 (2015) 167–175. doi:10.1093/rb/rbv014.

[12] ISO 23317:2012 Implants for surgery - In vitro evaluation for apatite-forming ability of implant materials. https://www.iso.org/standard/54163.html/

[13] L. Han, A.J. Grodzinsky, C. Ortiz, Nanomechanics of the Cartilage Extracellular Matrix, Annu. Rev. Mater. Res. 41 (2011) 133–168. doi:10.1146/annurev-matsci-062910-100431.
[14] G. Cama, S. Nkhwa, B. Gharibi, A. Lagazzo, R. Cabella, C. Carbone, P. Dubruel, H. Haugen, L. Di Silvio, S. Deb, The role of new zinc incorporated monetite cements on osteogenic differentiation of human mesenchymal stem cells, Mater. Sci. Eng. C. 78 (2017) 485–494. doi:10.1016/j.msec.2017.04.086.
[15] C. Vaquette, S. Saifzadeh, A. Farag, D.W. Hutmacher, S. Ivanovski, Periodontal Tissue Engineering with a Multiphasic Construct and Cell Sheets, J. Dent. Res. 98 (2019) 673–681. doi:10.1177/0022034519837967.
[16] E.M. Varoni, S. Vijayakumar, E. Canciani, A. Cochis, L. De Nardo, G. Lodi, L. Rimondini, M. Cerruti, Chitosan-Based Trilayer Scaffold for Multitissue Periodontal Regeneration, J. Dent. Res. 97 (2018) 303–311. doi:10.1177/0022034517736255.
[17] S. Sowmya, U. Mony, P. Jayachandran, S. Reshma, R.A. Kumar, H. Arzate, S.V. Nair, R. Jayakumar, Tri-Layered Nanocomposite Hydrogel Scaffold for the Concurrent Regeneration of Cementum, Periodontal Ligament, and Alveolar Bone, Adv. Healthc Mater. 6 (2017). doi:10.1002/adhm.201601251.
[18] Y. Zhang, X. Zhang, B. Shi, R. Miron, Membranes for guided tissue and bone regeneration, Oral and Maxillofacial Surgery. 1 (2013) 1–10. doi:10.13172/2052-7837-1-1-451.
[19] J. Li, J. Yang, J. Li, L. Chen, K. Liang, W. Wu, X. Chen, J. Li, Bioinspired intrafibrillar mineralization of human dentine by PAMAM dendrimer, Biomaterials. 34 (2013) 6738–6747. doi:10.1016/j.biomaterials.2013.05.046.
[20] R. Osorio, E. Osorio, A.L. Medina-Castillo, M. Toledano, Polymer Nanocarriers for Dentin Adhesion, J. Dent. Res. 93 (2014) 1258–1263. doi:10.1177/0022034514551608.
[21] S. Ferraris, S. Yamaguchi, N. Barbani, M. Cazzola, C. Cristallini, M. Miola, E. Vernè, S. Spriano, Bioactive materials: In vitro investigation of different mechanisms of hydroxyapatite precipitation, Acta Biomater. 102 (2020) 468–480. doi:10.1016/j.actbio.2019.11.024.
[22] A.M. Pietak, J.W. Reid, M.J. Stott, M. Sayer, Silicon substitution in the calcium phosphate bioceramics, Biomaterials. 28 (2007) 4023–4032. doi:10.1016/j.biomaterials.2007.05.003.
[23] C.Q. Ning, J. Mehta, A. El-Ghannam, Effects of silica on the bioactivity of calcium phosphate composites in vitro, J. Mater. Sci. Mater. Med. 16 (2005) 355–360. doi:10.1007/s10856-005-0635-8.
[24] K. Rezwan, Q.Z. Chen, J.J. Blaker, A.R. Boccaccini, Biodegradable and bioactive porous polymer/inorganic composite scaffolds for bone tissue engineering, Biomaterials. 27 (2006) 3413–3431. doi:10.1016/j.biomaterials.2006.01.039.
[25] Y.C. Chai, A. Carlier, J. Bolander, S.J. Roberts, L. Geris, J. Schrooten, H. Van Oosterwyck, F.P. Luyten, Current views on calcium phosphate osteogenicity and the translation into effective bone regeneration strategies, Acta Biomater. 8 (2012) 3876–3887. doi:10.1016/j.actbio.2012.07.002.
[26] G.R. Beck, Inorganic phosphate as a signaling molecule in osteoblast differentiation, J. Cell. Biochem. 90 (2003) 234–243. doi:10.1002/jcb.10622.
[27] G.E. Breitwieser, Extracellular calcium as an integrator of tissue function, Int. J. Biochem. Cell Biol. 40 (2008) 1467–1480. doi:10.1016/j.biocel.2008.01.019.

[28] I. Bružauskaitė, D. Bironaitė, E. Bagdonas, E. Bernotienė, Scaffolds and cells for tissue regeneration: different scaffold pore sizes-different cell effects, Cytotechnology. 68 (2016) 355–369. doi:10.1007/s10616-015-9895-4.
[29] K.M. Woo, V.J. Chen, P.X. Ma, Nano-fibrous scaffolding architecture selectively enhances protein adsorption contributing to cell attachment, J. Biomed. Mater. A. 67A (2003) 531–537. doi:10.1002/jbm.a.10098.
[30] T. Ramon-Marquez, A.L. Medina-Castillo, A. Fernandez-Gutierrez, J.F. Fernandez-Sanchez, A novel optical biosensor for direct and selective determination of serotonin in serum by Solid Surface-Room Temperature Phosphorescence, Biosens. Bioelectron. 82 (2016) 217–223. doi:10.1016/j.bios.2016.04.008.
[31] M. Toledano, M. Toledano-Osorio, E. Guerado, E. Caso, E. Osorio, R. Osorio, Assessing bone quality through mechanical properties in postmenopausal trabecular bone, Injury. 49 Suppl 2 (2018) S3–S10. doi:10.1016/j.injury.2018.07.035.
[32] A.J. Engler, S. Sen, H.L. Sweeney, D.E. Discher, Matrix elasticity directs stem cell lineage specification, Cell. 126 (2006) 677–689. doi:10.1016/j.cell.2006.06.044.
[33] B.M. Baker, B. Trappmann, W.Y. Wang, M.S. Sakar, I.L. Kim, V.B. Shenoy, J.A. Burdick, C.S. Chen, Cell-mediated fibre recruitment drives extracellular matrix mechanosensing in engineered fibrillar microenvironments, Nat. Mater. 14 (2015) 1262–1268. doi:10.1038/nmat4444.
[34] H.H. Winter, Can the gel point of a cross-linking polymer be detected by the G′ – G″ crossover?, Polym. Eng. Sci. 27 (1987) 1698–1702. doi:10.1002/pen.760272209.
[35] B. Xu, M.-J. Chow, Y. Zhang, Experimental and Modeling Study of Collagen Scaffolds with the Effects of Crosslinking and Fiber Alignment, International Journal of Biomaterials. (2011) 1–12. doi:10.1155/2011/172389.
[36] R. Agrawal, A. Nieto, H. Chen, M. Mora, A. Agarwal, Nanoscale damping characteristics of boron nitride nanotubes and carbon nanotubes reinforced polymer composites, ACS Appl. Mater. Interfaces. 5 (2013) 12052–12057. doi:10.1021/am4038678.
[37] J.M. Sadowska, F. Wei, J. Guo, J. Guillem-Marti, M.-P. Ginebra, Y. Xiao, Effect of nano-structural properties of biomimetic hydroxyapatite on osteoimmunomodulation, Biomaterials. 181 (2018) 318–332. doi:10.1016/j.biomaterials.2018.07.058.
[38] M.C. Bottino, R.A. Arthur, R.A. Waeiss, K. Kamocki, K.S. Gregson, R.L. Gregory, Biodegradable nanofibrous drug delivery systems: effects of metronidazole and ciprofloxacin on periodontopathogens and commensal oral bacteria, Clin. Oral Investig. 18 (2014) 2151–2158. doi:10.1007/s00784-014-1201-x.
[39] Z. Chen, A. Bachhuka, S. Han, F. Wei, S. Lu, R.M. Visalakshan, K. Vasilev, Y. Xiao, Tuning Chemistry and Topography of Nanoengineered Surfaces to Manipulate Immune Response for Bone Regeneration Applications, ACS Nano. 11 (2017) 4494–4506. doi:10.1021/acsnano.6b07808.

Figure 1. Zinc chelation ability **a)** and doxycycline doping values **b)** on experimental membranes. Determinations were performed in triplicate.

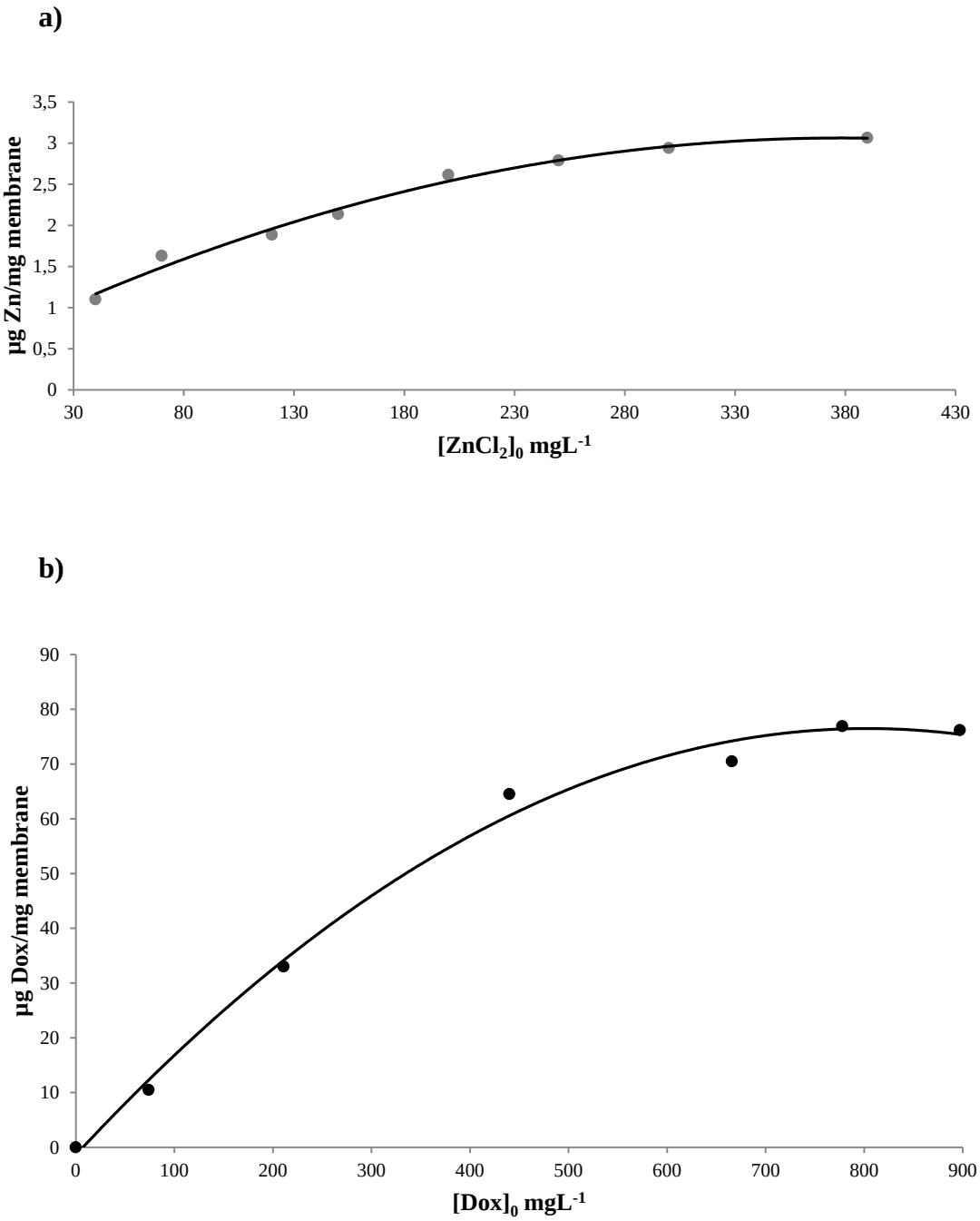

Figure 2. AFM images of the membranes surfaces **a)** COOH-Membrane, **b)** COOH-Si-Membrane, **c)** Zn-Si-Membrane and **d)** Dox-Si-Membrane. Overlapped and randomly distributed nanofibers may be observed. All surfaces presented similar morphology.

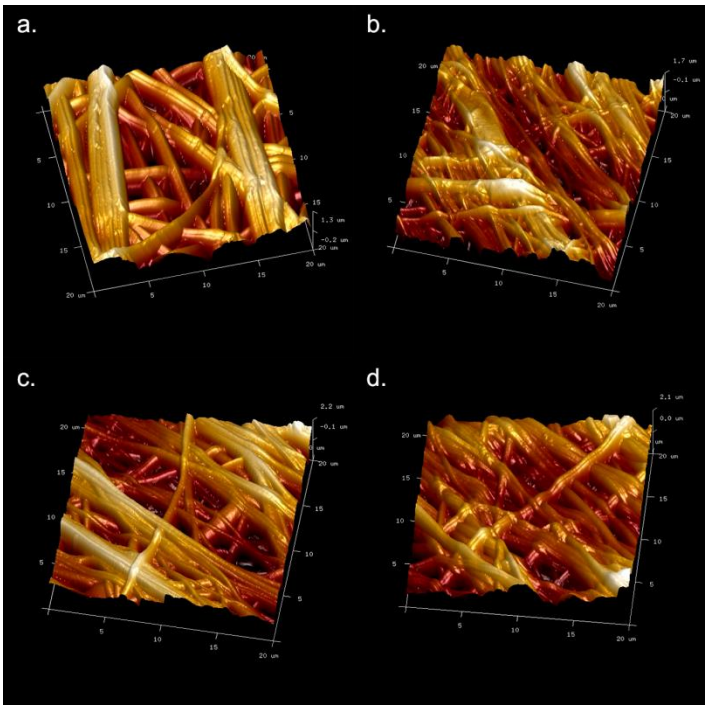

Figure 3. FESEM micrographs of membranes after SBF immersion over 7 days are presented in: **a)** COOH-Membrane where very few or no rounded mineral deposits were observed, **b)** COOH-Si-Membrane, **c)** Zn-Si-Membrane and **d)** Dox-Si-Membrane. Nanofibers lost their smooth appearance. Mineral deposits were uniformly distributed throughout nanofiber surfaces (**b, c** and **d**). Calcium and phosphate were identified after EDX analysis of silica loaded membranes (**Ep1**, **Ep2**, **Ep3 and Ep4** correspond to images **a, b, c** and **d** respectively). Silicon is also present at the EDX spectra. Magnesium and aluminum are contaminant elements from the sample holder.

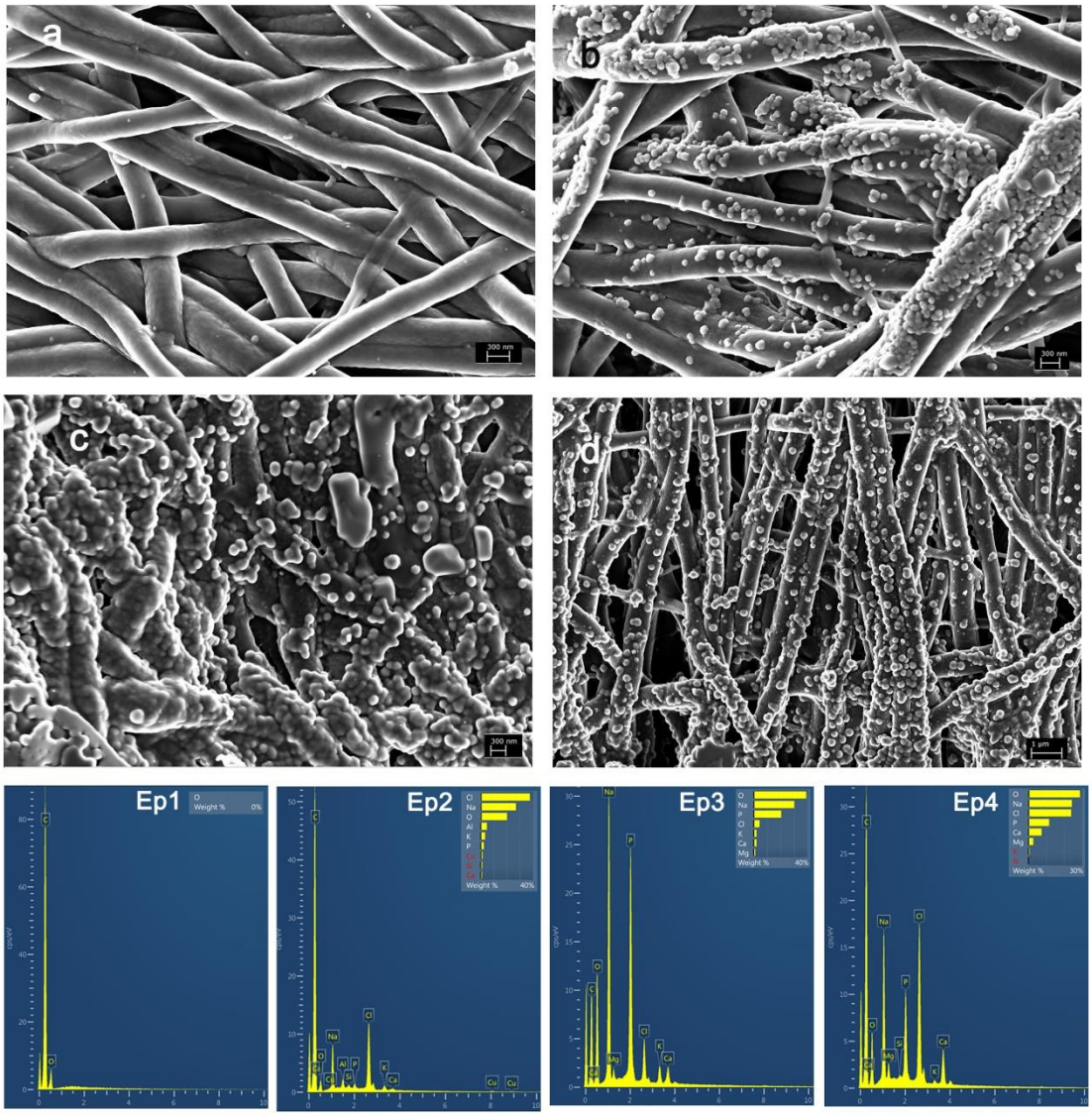

Figure 4. Nano-DMA analysis, on scanning mode, of the membrane surfaces **a)** COOH-Membrane, **b)** COOH-Si-Membrane, **c)** Zn-Si-Membrane and **d)** Dox-Si-Membrane. Properties maps correspond to complex (*E**), loss (*E*), storage modulus (*E'*) and tan Delta (δ). Scanned areas are 20 x 20 μm. Scale bars correspond to values in GPa.

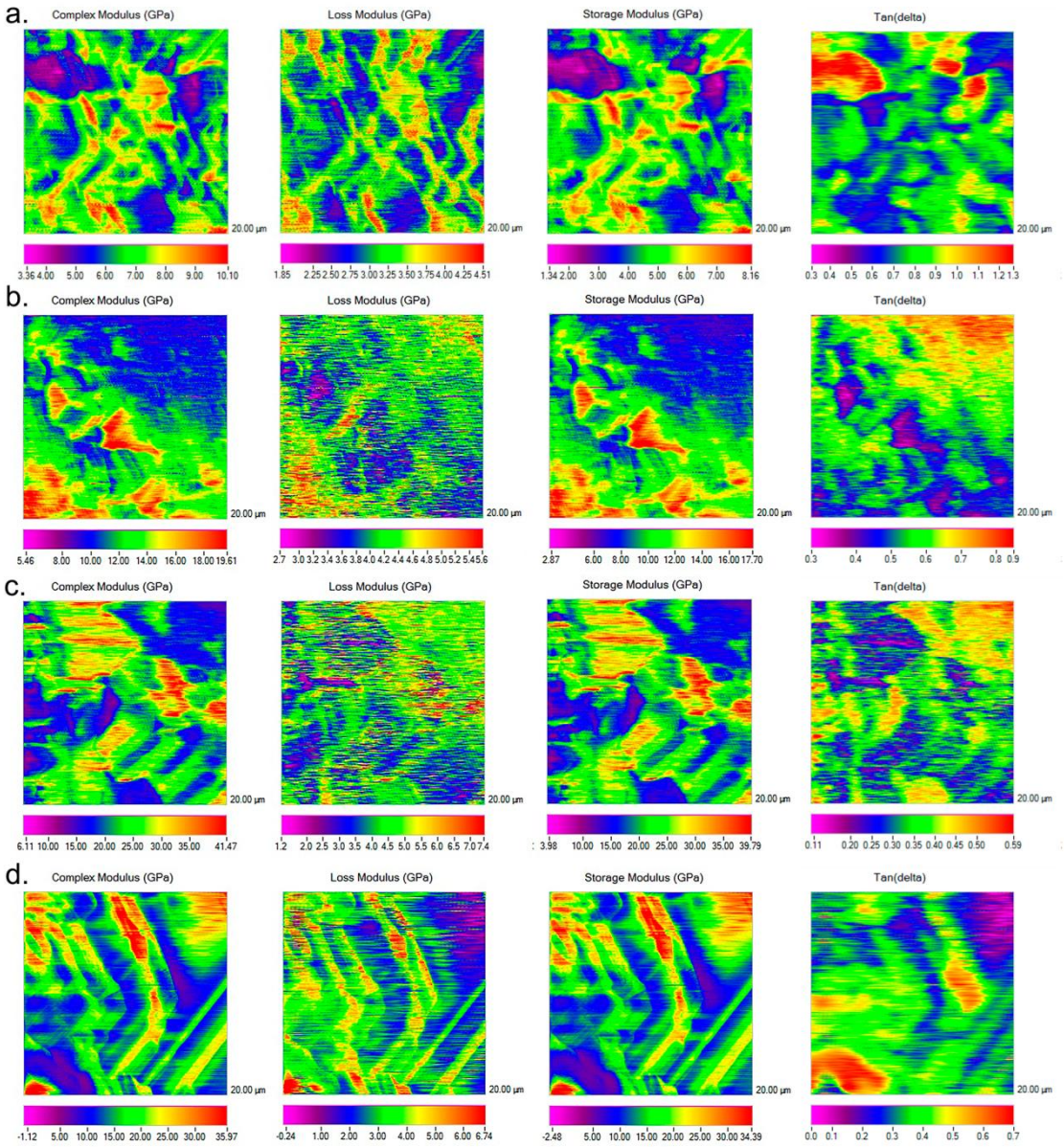

Figure 5. Fluorescence mean values and standard deviations obtained after the Alamar blue test for the different membranes. 1.6 x 10^6 HOS TE85 human osteosarcoma cells were seeded per membrane and cultured until the different time-points. Osteogenic inducers were not added to the media. Experiments were performed in triplicate. Same capital letter indicates no significant difference between membranes after 1 day culture. Same low-case letters indicate no difference between membranes after 3 days culture. Same symbols indicate no difference between membranes after 7 days culture. Numbers indicate differences between time-points, considering the same membrane. Student Newman Keuls multiple comparisons were significant if $p<0.05$.

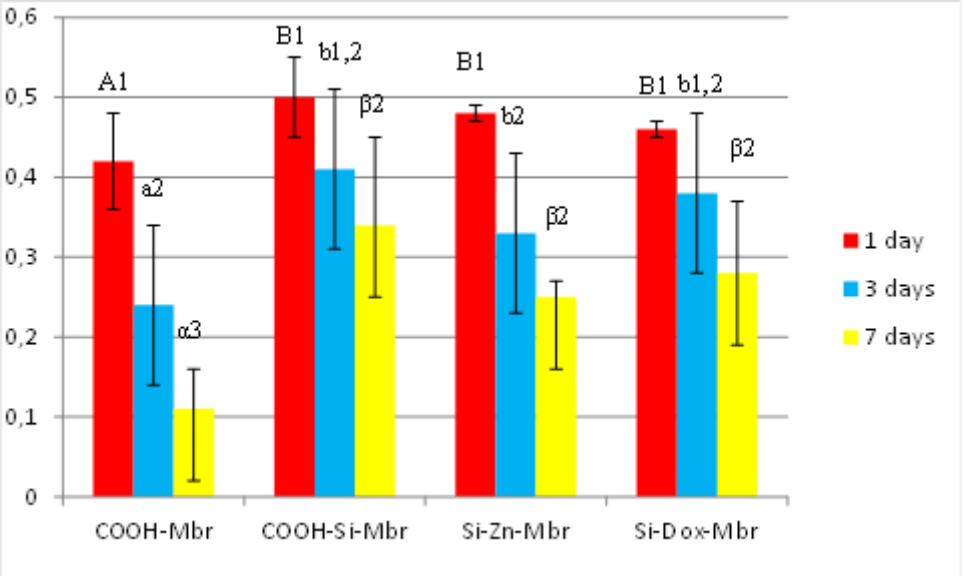

Figure 6. Surface FESEM images of the experimental membranes seeded with osteoblasts cells and cultured for 24 h, 7 and 14 days. 1.6 x 10^6 HOS TE85 human osteosarcoma cells were seeded per tissue. Cells were cultured without osteogenic inducers. Following images correspond to cells on COOH-Membranes after: **a)** 24h, some flat and elongated cells are observed on the membrane (pointers). Long osteoblasts filapodia may be observed crossing over the membranes surfaces (arrows), they are thicker than fibers from membranes; **b)** 7d, at higher magnification an osteoblast covered by extracellular substance is observed (pointer) filapodia are intermingled with membranes fibers (arrow); and **c)** 14d, several aligned osteoblast connected each other may be seen (pointers), numerous filapodia are detected on the surface (arrows). Following images correspond to cells on COOH-Si-Membranes after: **d)** 24h, at high magnification several osteoblasts, confluence between them is clear (pointers), many filapodia emerging from osteoblasts cytoplasm are also observable (arrows); **e)** 7d, osteoblasts are detected on the membrane surface (pointers), they are partially covered by fibrilar substance and filapodia (arrows), some mineral deposits may also be seen (double arrows); and **f)** 14d, osteoblast cells are covered by mineral deposits (double arrows), tiny crystals may also been observed onto the surface (arrow heads). Following images correspond to cells on Zn-Si-Membrane after: **g)** 24h, large osteoblasts are observed (pointers) and are confluence between each other, filapodia emerging from cells cytoplasm are visible (arrows), some mineral deposits are detected on the membrane surface (arrowhead); **h)** 7d large osteoblasts (pointers) with numerous filapodia (arrows) at close contact with membranes and deep inside them are encountered; and **i)** 14d, some osteoblasts may be seen (pointer), but most of them are covered by fibrilar substance and mineral deposits with crystals (arrowheads) osteoblasts appeared completely covered by this new produced mineralized material. Last images correspond to cells on Dox-Si-Membrane after: **j)** 24h, large osteoblasts cells (pointers) with thick filapodia (arrows) are detected on the membrane surfaces; **k)** 7d, osteoblasts cells which are partially covered by fibrilar substance are seen (pointers), mineral deposits (double arrow) and crystals (arrowhead) are also observed; and **l)** 14d, cells are attached to the surface of membranes (pointers), cells were producing plenty of extracellular matrix and fibrils, which in some cases were not easy to distinguish from membrane's nanofibers, fibers produced by osteoblasts were partially or completely covering the cells, tiny crystals were scattered onto the cell membranes or onto the new produced fibers (arrowheads). When silica was present in membranes composition, cell attachment and spreading, fiber production and minerals deposition were enhanced.

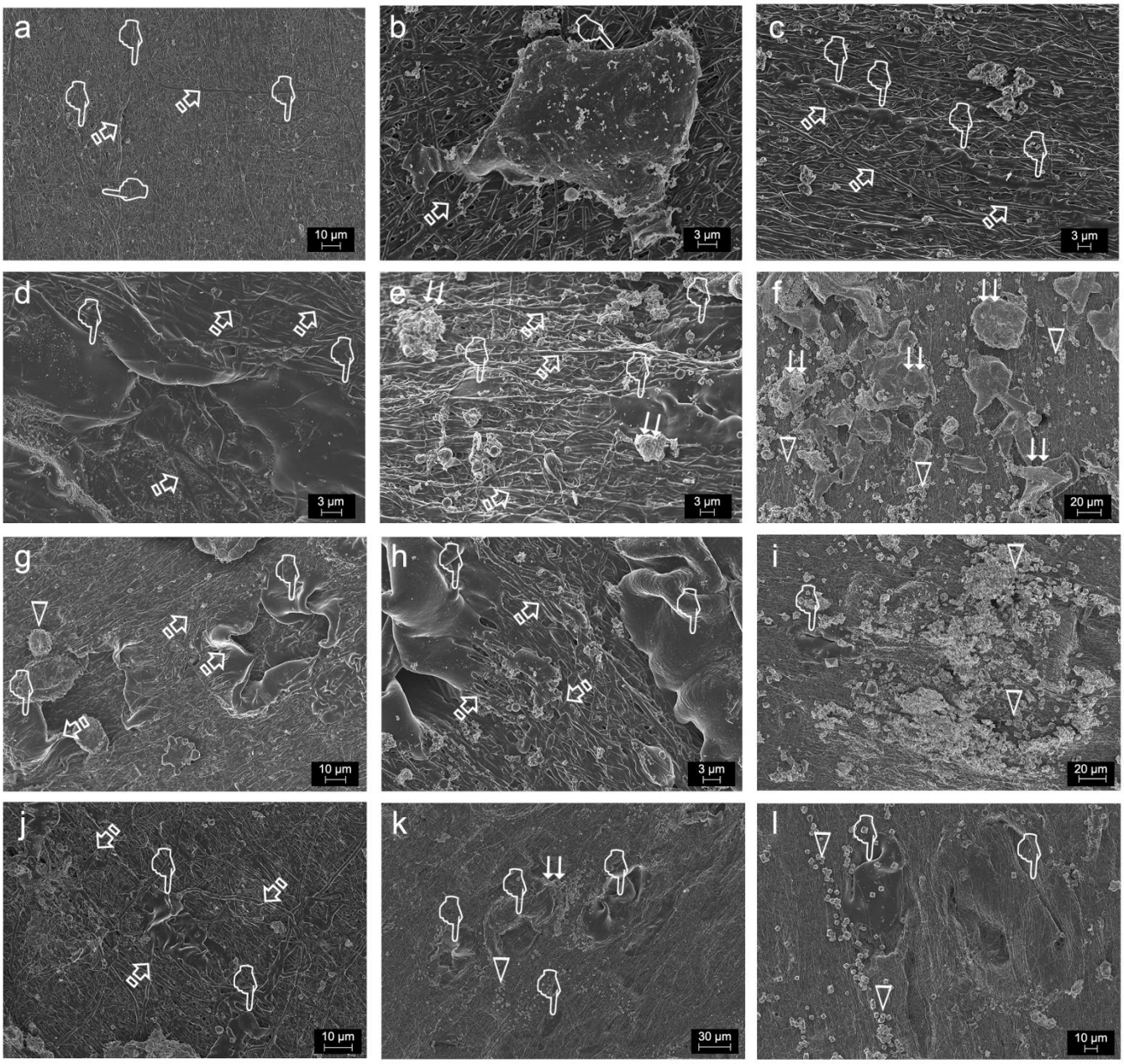
a
10 µm
b
3 µm
c
3 µm
d
3 µm
e
3 µm
f
20 µm
g
10 µm
h
3 µm
i
20 µm
j
10 µm
k
30 µm
l
10 µm